Label inspection of approximate cylinder based on adverse cylinder panorama

Lin, Jianping, Liao, Qingmin, He, Bei, Shi, Chenbo

Jianping Lin, Qingmin Liao, Bei He, Chenbo Shi, "Label inspection of approximate cylinder based on adverse cylinder panorama," Proc. SPIE 9045, 2013 International Conference on Optical Instruments and Technology: Optoelectronic Imaging and Processing Technology, 90451Y (19 December 2013); doi: 10.1117/12.2042075

Event: International Conference on Optical Instruments and Technology (OIT2013), 2013, Beijing, China

Label inspection of approximate cylinder based on adverse cylinder panorama

Jianping Lin[a], Qingmin Liao[a], Bei He[b], Chenbo Shi[b]

[a] Shenzhen Key Lab. of Information Sci&Tech/Shenzhen Engineering Lab. of IS&DRM, Department of Electronic Engineering/Graduate School at Shenzhen, Tsinghua University

[b] Department of Electronic Engineering, Tsinghua University, China

ABSTRACT

This paper presents a machine vision system for automated label inspection, with the goal to reduce labor cost and ensure consistent product quality. Firstly, the images captured from each single-camera are distorted, since the inspection object is approximate cylindrical. Therefore, this paper proposes an algorithm based on adverse cylinder projection, where label images are rectified by distortion compensation. Secondly, to overcome the limited field of viewing for each single-camera, our method novelly combines images of all single-cameras and build a panorama for label inspection. Thirdly, considering the shake of production lines and error of electronic signal, we design the real-time image registration to calculate offsets between the template and inspected images. Experimental results demonstrate that our system is accurate, real-time and can be applied for numerous real-time inspections of approximate cylinders.

Keywords: image mosaicing, label inspection, adverse cylinder projection, image registration

1. INTRODUCTION

Label inspection has attracted much interest in image processing and compute vision recently, which can benefit industrial inspection greatly. The usual defects in label inspection include no-label, wrong-label, broken-label and skewed-label. Traditional manual inspection confronts problems such as high complexity and financial cost. With the continuous development of image processing technology and the decrease of the hardware prices, a growing number of machine vision systems have been applied in such industrial inspection applications.[1] Compared to manual inspection, machine vision systems have great advantages in terms of cost, standardization and inspection speed.

Recent algorithms concentrated on inspecting defects via comparing features between template and inspected images. However, there exist two problems. On one hand, due to limited field of viewing for each single-camera, many small defects cannot be inspected so that the accuracy is affected significantly. On the other hand, due to the shake of production lines and error of electronic signal, the template and inspected images are shifted. Thus, directly matching would result in inspection errors. To deal with problems mentioned above, this paper proposes an adverse cylinder mosaic system for label inspection of approximate cylinders. By using adverse cylinder projection, the rectified image of each single-camera can be obtained. And then all rectified images are combined by the image mosaicing algorithm based on SIFT(Scale Invariant Feature Transform).[2] Finally, an effective inspection method is carried on the panorama of the label to detect whether there exists any defect.

The rest of this paper is organized as follow. In section 2 the mechanical part of the label inspection system is described, followed by a description about the calibration process of the system. In section 3, the algorithm for the adverse cylinder projection and image mosaicing are described. Experimental work is conducted in Section 4, and finally conclusions are discussed in section 5.

Further author information: (Send correspondence to Bei He)
E-mail: thu-hebei@163.com, Telephone: +86 1 391 1853 486

2013 International Conference on Optical Instruments and Technology: Optoelectronic Imaging and Processing Technology, edited by Xinggang Lin, Jesse Zheng, Proc. of SPIE Vol. 9045, 90451Y
 · doi: 10.1117/12.2042075

2. THE LABEL INSPECTION SYSTEM

2.1 Machine Vision System

As shown schematically in figure 1, the complete label inspection system consists of a conveyor unit, a vision unit and a rejection unit. When performing inspection, the conveyor transports the beverage bottle towards the vision unit where the inspection takes place. In order to guarantee a full view of the beverage, 4 color CCD cameras are placed symmetrically with respect to the bottle. The trigger will generate a signal when a bottle passing by, which informs cameras to grab images simultaneously. And then the images grabbed would be sent to IPC(Industrial Personal Computer) for inspection. The inspection result will be sent to the controller to guide the rejecter to take corresponding measure. Before inspection start, the system must be calibrated. We will describe the calibration process in the next chapter. During the calibration phase, we should adjust the camera position to ensure that the bottle is located in the center of the camera view field.

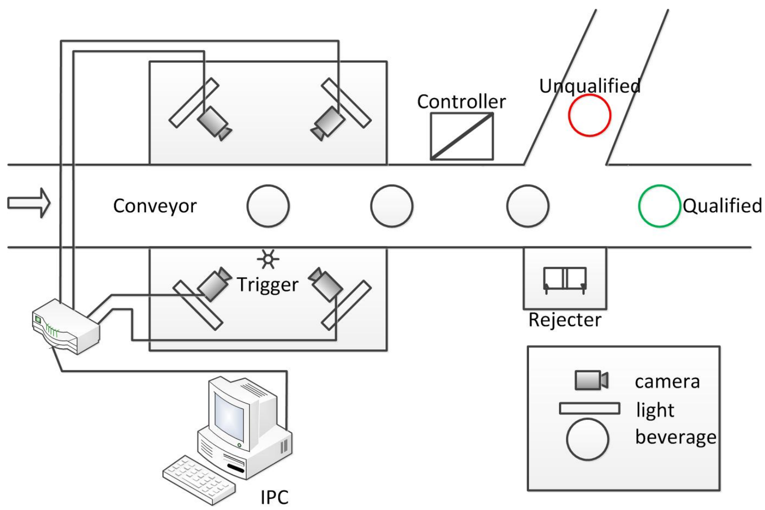

Figure 1. Schematic diagram of the label inspection system

2.2 Camera Calibration

Camera calibration in the context of three-dimensional machine vision is the process of determining the internal camera geometric and optical characteristics (intrinsic parameters) and/or the 3-D position and orientation of the camera frame relative to a certain world coordinate system (extrinsic parameters).[3] The calibration process is performed with the "camera calibration toolbox for matlab"*. For each single-camera, we grab a total of 20 images of the planar checkerboard and use the calib_gui module to calculate the intrinsic parameters. The list of internal parameters include the focal length stored in a $2*1$ vector $\boldsymbol{fc}$, the principal point stored in a $2*1$ vector $\boldsymbol{cc}$, the skewed coefficient stored in the scalar $\boldsymbol{alpha\_c}$ and the distortions stored in the $5*1$ vector $\boldsymbol{kc}$. For each pair of two adjacent cameras, 20 pairs of corresponding left and right images are captured to calculate the extrinsic parameters $\boldsymbol{om}$ and $\boldsymbol{T}$. $\boldsymbol{om}$ and $\boldsymbol{T}$ are defined such that if we consider a point $\boldsymbol{p}$ in 3D space, coordinate vectors $\boldsymbol{X_l}$ and $\boldsymbol{X_r}$ in the left and right camera reference frames respectively are related to each other through the rigid motion transformation $\boldsymbol{X_r} = \boldsymbol{R^{-1}} * \boldsymbol{X_l} + \boldsymbol{T}$, where $\boldsymbol{R}$ is the $3*3$ rotation matrix corresponding to the rotation vector $\boldsymbol{om}$. The relation between $\boldsymbol{om}$ and $\boldsymbol{R}$ is given by the rodrigues formula $\boldsymbol{R} = \boldsymbol{rodrigues(om)}^{\dagger}$.

2.3 Bottle Location Calibration

In order to obtain the adverse cylinder projection model, the positional relationship between the cameras and the bottle should be calibrated.The captured images are shown in Figure 2(a), 2(b) and the mask images extracted are shown in Figure 2(c), 2(d). we denote the image coordinates of point $\boldsymbol{P_l}$ which is located in the 1/2 height

*More details refer to http://www.vision.caltech.edu/bouguetj/calib_doc/

†More details refer to http://www.vision.caltech.edu/bouguetj/calib_doc/htmls/example5.html

and 1/2 width of the left mask as (u_l, v_l). Similarly the image coordinates (u_r, v_r) of corresponding point $\boldsymbol{P_r}$ in the right mask image can be obtained.

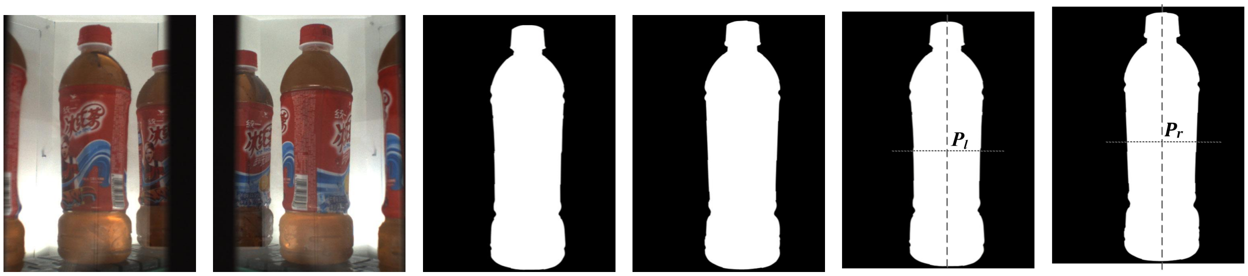

(a) left image (b) right image (c) left Mask (d) right Mask (e) center point P_l (f) center point P_r

Figure 2. Camera images, mask images and the center points of left and right mask

According to the projection relationship, we can infer that point $\boldsymbol{P_l}$ and $\boldsymbol{P_r}$ are the projection points of the same point $\boldsymbol{P}$ in the left and right camera imaging plane. (X_l, Y_l, Z_l) and (X_r, Y_r, Z_r) are the coordinate vectors of $\boldsymbol{P}$ in the left and camera frame. Thus the relationship between camera coordinates (X_l, Y_l, Z_l) and image coordinates (u_l, v_l) can be performed by using the following equation:

$$\begin{bmatrix} u_l \\ v_l \\ 1 \end{bmatrix} = \begin{bmatrix} fc_x & 0 & cc_x \\ 0 & fc_y & cc_y \\ 0 & 0 & 1 \end{bmatrix} \begin{bmatrix} X_l/Z_l \\ Y_l/Z_l \\ 1 \end{bmatrix} \tag{1}$$

Where fc_x,fc_y,cc_x,cc_y are the intrinsic parameters of the left camera.

By solving Equation (1), the parametric equation of the ray which is out from the optical center of left camera and passes through point $\boldsymbol{P}$ can be written as follow:

$$\begin{bmatrix} X_l/Z_l \\ Y_l/Z_l \end{bmatrix} = \begin{bmatrix} l_x \\ l_y \end{bmatrix} \tag{2}$$

Similarly, another ray equation with regard to (X_r, Y_r, Z_r) can be written in the following form:

$$\begin{bmatrix} X_r/Z_r \\ Y_r/Z_r \end{bmatrix} = \begin{bmatrix} r_x \\ r_y \end{bmatrix} \tag{3}$$

According to the rigid motion transformation, (X_l, Y_l, Z_l) and (X_r, Y_r, Z_r) should conform to the following matrix equation:

$$\begin{bmatrix} X_r \\ Y_r \\ Z_r \end{bmatrix} = R^{-1} * \begin{bmatrix} X_l \\ Y_l \\ Z_l \end{bmatrix} + \begin{bmatrix} T_x \\ T_y \\ T_z \end{bmatrix} \tag{4}$$

Denote $\boldsymbol{R^{-1}}$ as $\boldsymbol{Q}$ where

$$Q = \begin{bmatrix} q_{11} & q_{12} & q_{13} \\ q_{21} & q_{22} & q_{23} \\ q_{31} & q_{32} & q_{33} \end{bmatrix}$$

Combining Eqs. (2), (3), (4), an unified equation can be obtained as the following expression:

$$\begin{bmatrix} q_{11} - r_x q_{31} & q_{12} - r_x q_{32} & q_{13} - r_x q_{33} \\ q_{21} - r_y q_{31} & q_{22} - r_y q_{32} & q_{23} - r_y q_{33} \\ 1 & 0 & l_x \\ 0 & 1 & l_y \end{bmatrix} \begin{bmatrix} X_l \\ Y_l \\ Z_l \end{bmatrix} = \begin{bmatrix} T_x - r_x T_z \\ T_y - r_y T_z \\ 0 \\ 0 \end{bmatrix} \tag{5}$$

By solving Equation (5), the camera coordinates of point $\boldsymbol{P}$ related to the left frame can be calculated. Thus the radius of the bottle R and the distance between the camera optical center and the bottle center d can be calibrated.

3. ALGORITHM DESIGN

3.1 Adverse Cylinder Projection

As shown in figure 2(a), the images captured from each single-camera would been distorted in both X-axis and Y-axis direction. Wherein the distortion in X-axis direction is mainly due to the cylindrical shape of the bottle and the distortion in Y-axis direction is mainly caused by the perspective distortion. Since the causes of these two distortion are irrelevant, thus we can perform the distortion compensation process separately.

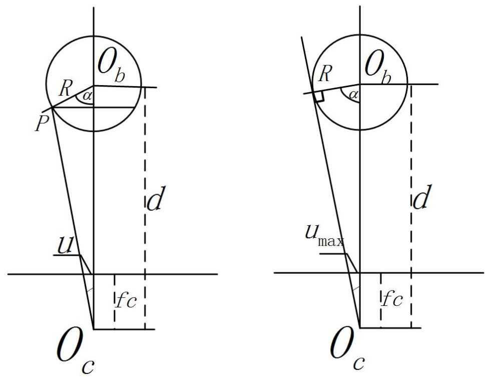

Figure 3. Schematic diagram for distortion in X-axis direction

A schematic diagram for distortion in X-axis direction is shown in Figure 3. Denote u as the X-axis image coordinate of point $\boldsymbol{P}$ and α as the angle between line $\overline{\boldsymbol{O_b P}}$ and $\overline{\boldsymbol{O_b O_c}}$. According to the properties of similar triangles, the following equation can be derived:

$$\frac{u}{fc} = \frac{R\sin\alpha}{d - R\cos\alpha} \tag{6}$$

Where fc,R,d are the results of the calibration process.

Let u_{max} be the distance between the boundary and the central axis of bootle image in imaging plane, thus u_{max} conforms to the following equation:

$$\frac{u_{max}}{fc} = \frac{R}{\sqrt{d^2 - R^2}} \tag{7}$$

Combining Eqs. (6), (7), the transformation formula between u and α can be expressed as:

$$u = u_{max} \cdot \frac{\sqrt{d^2 - R^2}\sin\alpha}{d - R\cos\alpha} \tag{8}$$

According to the pinhole camera model, the distortion of Y-axis coordinate can be modeled as an ellipse. Length of the long axis $\boldsymbol{a}$ is equal to u_max. As shown in Figure 4, point $\boldsymbol{P_f}$ and $\boldsymbol{P_b}$ are in the same height of the bottle where $\boldsymbol{P_f}$ is the point closest to the camera and $\boldsymbol{P_b}$ is the furthest. Thus the Y-axis image coordinates of point $\boldsymbol{P_f}$ and $\boldsymbol{P_b}$, denoted as v_f and v_b, would conform to the follow equations:

$$\frac{v_f}{fc} = \frac{v_{max}}{d - R} \qquad \frac{v_b}{fc} = \frac{v_{max}}{d + R} \tag{9}$$

Therefore length of the short axis, denoted as $\boldsymbol{b}$, can be calculated as follow:

$$b = v_f - v_b = v_{max} \cdot \frac{R}{d + R} \tag{10}$$

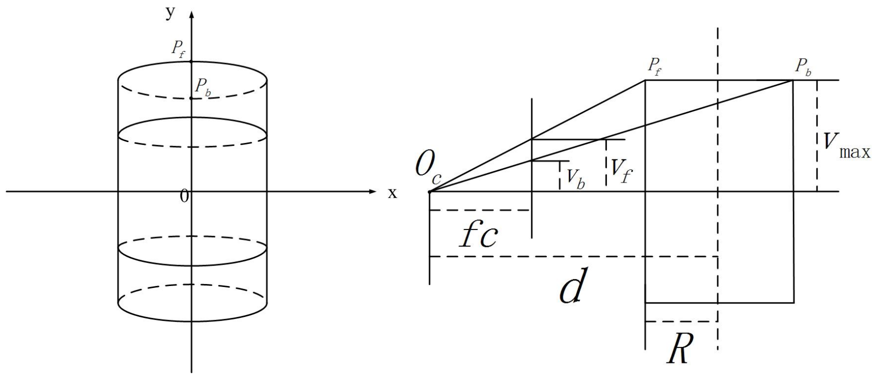

Figure 4. Schematic diagram for distortion in Y direction

According to the elliptic equation, the transformation formula between v and α is obtained:

$$v = b\sqrt{1-\frac{u^2}{a^2}} = v_{max}\cdot\frac{R}{d+R}\cdot\sqrt{1-\frac{(d^2-R^2)\sin^2\alpha}{(d-R\cos\alpha)^2}} \tag{11}$$

We put $(\alpha+90)$ as the new X-axis coordinate of the result image. For each point in the result image, the corresponding coordinates in the original image can be calculated by Eqs. (8) and (11). Thus, the distorted image can be expanded by angle. For coordinates which can not be located in the original image, bilinear interpolation would be performed to get the pixel's value.

3.2 Image Mosaicing

The image mosaicing process[4] consists of image acquisition, feature points extraction and matching, image registration[5,6] and image fusion. In our algorithm, the inputs of the image acquisition module are the rectified images after adverse cylinder projection. Considering the performance of different features[7] in handling challenges such as scale changes, image rotation and illumination changes, we select SIFT as the feature to find correspondences in the images. For each pair of adjacent images, SIFT feature points are extracted in both. And then the best candidate match for each feature point is found by identifying its nearest neighbor in the data set of feature vectors.[8] Thus the homograph between the two images[9] can be calculated by using the correspondence data. The homograph is a mapping between two perspective images, typically a 3*3 matrix which conforms to the following equation:

$$\lambda\begin{bmatrix} x^{'} \\ y^{'} \\ 1 \end{bmatrix} = \begin{bmatrix} h_{11} & h_{12} & h_{13} \\ h_{21} & h_{22} & h_{23} \\ h_{31} & h_{32} & h_{33} \end{bmatrix}\begin{bmatrix} x \\ y \\ 1 \end{bmatrix} \tag{12}$$

However, erroneous result of homograph may be given when incorrect registration points occurred. In order to solve this problem, the RANSAC(RANdom Sample Consensus) algorithm[10] is used to obtain the correct homograph $\boldsymbol{H}$ which is consistent with the inliers and rejects outliers in the same time. Once the best homograph $\boldsymbol{H}$ has been found, we can blend these two images together. Finally, to reduce visible artifacts, a weighting function is proposed to blur the edges of the component images, written in the following form:

$$f(x,y) = \begin{cases} f_1(x,y) & (x,y)\in f_1 \\ k_1 f_1(x,y) + k_2 f_2(x,y) & (x,y)\in(f_1\cap f_2) \\ f_2(x,y) & (x,y)\in f_2 \end{cases} \tag{13}$$

Where f_1, f_2 are the two adjacent images and f is the mosaic image. k_1, k_2 is the weighted value and $k_1+k_2=1$, $0\le k_1,k_2\le 1$.

3.3 Defect Inspection

In order to handle the mismatch problem caused by the rotation of the bottle, firstly we should calculate the offset between the template and the inspected image. For this purpose, a sub-block image is extracted from the inspected image. And then we calculate the location of the sub-block in the template image by template matching. Thus the offset between the template and the inspected image can be obtained. The inspected image would then be rotated according to the offset. And that we divide the rotated image into small blocks. For each block, a feature vector which contains the values of local descriptors such as HOG,[11] color histogram and haar-like features would be calculated. Finally, we calculate the similarity measurement between the same sub-block of the template and the inspected image. If the difference is greater than a threshold, thus we can classify the inspected image as a default label.

4. EXPERIMENTAL RESULTS

The algorithm has been implemented in vs2008 and all experiments have been carried out on a Nuvo-1005b IPC, core i5 540M and 2G RAM. The input images are shown in Figure 5 and the corresponding inspection result is shown in Figure 6.

Figure 5. Images captured

Figure 6. The inspection result of label image

To evaluate the performance of our algorithm, a large number of images are captured which include 10,000 static and 10,000 dynamic images.Due to the design of adverse cylinder panorama, we can amplify small defects so that the inspection accuracy increases significantly. We compare our results with ones calculated by single-camera inspection. The FN and FP of our algorithm are (0.07%, 0.01%) and (0.11%, 0.04%) respectively, where ones of single-camera inspection are (0.26%, 0.13%) and (0.47%, 0.28%). Experimental results demonstrate that our algorithm is accurate and real-time. Hence, our system can be applied for numerous inspections of approximate cylinders.

5. CONCLUSIONS

In this paper, an automatic label inspection system is proposed by using the adverse cylinder projection and image mosaicing. System is firstly be calibrated to obtain the position relationship between the cameras and the bottle, and then adverse cylinder projection is taken on each single-camera image to rectify the distorted image. After that the panorama of the label image is obtained by image mosaicing and inspection result is given by comparing with the template. Experimental results demonstrate that our algorithm is accurate and real-time, which can be applied for numerous real-time inspections of approximate cylinders.

ACKNOWLEDGMENTS

Partially supported by NSFC(No.61271390), national Science Fundation of China(No.61271393) and project of emerging industries of strategic importance of Shenzhen(NO.JCYJ2013040214500244).

REFERENCES

1. H. Golnabi and A. Asadpour, "Design and application of industrial machine vision systems," *Robotics and Computer-Integrated Manufacturing* **23**(6), pp. 630–637, 2007.
2. D. G. Lowe, "Distinctive image features from scale-invariant keypoints," *International journal of computer vision* **60**(2), pp. 91–110, 2004.
3. R. Tsai, "A versatile camera calibration technique for high-accuracy 3d machine vision metrology using off-the-shelf tv cameras and lenses," *Robotics and Automation, IEEE Journal of* **3**(4), pp. 323–344, 1987.
4. Y. Liu, G. Wang, A. Yao, H. Wang, and X. Lin, "Video mosaicking based on adaptive sampling," *Journal of Tsinghua University Science and Technology* **50**(1), pp. 108–112, 2010.
5. H. Bei, W. Guijin, L. Xinggang, and L. Chunxiao, "High-accuracy sub-pixel registration for noisy images based on phase correlation," *IEICE TRANSACTIONS on Information and Systems* **94**(12), pp. 2541–2544, 2011.
6. M. Quan, W. Guijin, and L. Xinggang, "Kernel based image registration incorporating with both feature and intensity matching," *IEICE TRANSACTIONS on Information and Systems* **93**(5), pp. 1317–1320, 2010.
7. K. Mikolajczyk and C. Schmid, "A performance evaluation of local descriptors," *Pattern Analysis and Machine Intelligence, IEEE Transactions on* **27**(10), pp. 1615–1630, 2005.
8. H. Zhou, Y. Yuan, and C. Shi, "Object tracking using sift features and mean shift," *Computer Vision and Image Understanding* **113**(3), pp. 345–352, 2009.
9. D. Gledhill, G. Y. Tian, D. Taylor, and D. Clarke, "Panoramic imaginga review," *Computers & Graphics* **27**(3), pp. 435–445, 2003.
10. M. A. Fischler and R. C. Bolles, "Random sample consensus: a paradigm for model fitting with applications to image analysis and automated cartography," *Communications of the ACM* **24**(6), pp. 381–395, 1981.
11. N. Dalal and B. Triggs, "Histograms of oriented gradients for human detection," in *Computer Vision and Pattern Recognition, 2005. CVPR 2005. IEEE Computer Society Conference on*, **1**, pp. 886–893, IEEE, 2005.